Robust Target Identification in White Gaussian Noise for Ultra Wide-Band Radar Systems

Jon E. Mooney, *Student Member, IEEE*, Zhi Ding, *Senior Member, IEEE*, and Lloyd S. Riggs, *Senior Member, IEEE*

***Abstract*— Radar target identification, as witnessed by the plethora of the literature on the topic, is an important problem of considerable interest to many civilian and military agencies. The number of signatures even for a small target library can become quite large since, in general, a unique return is produced for each new target aspect. Any robust target identification algorithm must adequately address this issue. The extinction pulse (E-pulse) and other related techniques, which are based on a singularity expansion method description of the radar return, indeed boast an aspect independent identification algorithm. However, as demonstrated in this paper, the performance of these techniques in white Gaussian noise is inferior to the method described here. In this paper, we develop a new method based on a generalized likelihood ratio test (GLRT) to perform target identification in the presence of white Gaussian noise. As with the E-pulse technique, our method takes advantage of the parsimonious singularity expansion representation of the radar return. In addition, sufficient statistics and simple practical implementations of a GLRT are presented. Simulation results using various thin wire targets are presented contrasting the performance of the GLRT to the E-pulse technique as a function of signal-to-noise (SNR) ratio.**

***Index Terms*— Noise, radar, radar target recognition, wideband radar.**

I. Introduction

In 1971, Baum [1] formalized a singularity expansion method (SEM) description for electromagnetic interaction or scattering problems in terms of simple poles (or singularities) in the complex frequency plane or correspondingly damped sinusoids in the time domain. Baum [2], [3] recently extended this earlier work to include the SEM description of scattered far fields. The SEM is used to write the late-time scattered field "impulse" response of a conducting body as a sum of complex exponential terms

$$r(t) = \sum_{i=1}^{N} a_i\, e^{(s_i\, t)}, \qquad t > T_L \tag{1}$$

where the complex amplitude coefficient (coupling coefficient) of the ith mode, a_i, depends on the orientation of the target with respect to the radar (aspect-dependent parameters). The pole term s_i is aspect-independent and represents the frequency and damping constant of the ith mode. Note that the summation is over poles and *not* over conjugate pole pairs. Thus, only $N/2$ modes are assumed excited by the incident field waveform. Late time, denoted by $t > T_L$, is defined as the time period after the incident pulse has passed over the target, so that subsequent radiation is associated with the target's free natural resonances. Equation (1) is constructed using what is referred to as a class I coupling coefficient [4]. An SEM representation for the scattered field employing a class II coupling coefficient may also be constructed and enjoys the advantage of greater accuracy than the class I form in early time $0 < t < T_L$ albeit at the expense of greater complexity [5].

Some early efforts [6] attempted to identify a target based on its unique aspect and excitation independent pole terms $(s = \xi + j\omega)$. Prony's method [7] was employed to extract poles from measured target pulse responses, but this approach met with limited success when the target responses were contaminated with noise.

In a more innovative approach, Rothwell *et al.* [8] and Chen *et al.* [9] employed extinction (E-pulse) and single mode extraction (S-pulse) waveforms to discriminate a given target response from among a group of such returns. This work is closely related to Kennaugh's kill (K-pulse) [10] which has been compared to the E-pulse method [11]. The aspect independent E-pulse and S-pulse are discriminatory waveforms which, when convolved with the late-time pulse response of a matched target, produce a null or single-mode responses, respectively. When an E-pulse tailored to one target is convolved with a different target a larger response results. The E- and S-pulses can be synthesized from knowledge of a target's poles or directly from measured target response data [12], [13] taken in a low-noise anechoic environment. Consequently, this discrimination scheme is inherently more robust than the previously mentioned direct pole-target matching approach. Ilavarasan *et al.* [14] recently automated the E-pulse and S-pulse discrimination schemes and provided an extensive analysis of how these schemes perform in the presence of noise.

The E- and S-pulse methods, though effective, represent only one particular utilization of the prior knowledge of a target's poles to discriminate among a set of targets. The noise effect on these two methods tend to seriously limit their performance. In this paper, we present a new and robust target discrimination method that is based on fundamental principles of detection and estimation theory, namely hypothesis testing.

Manuscript received August 26, 1996; revised August 25, 1997.
The authors are with the Department of Electrical Engineering, Auburn University, AL 36849 USA.
Publisher Item Identifier S 0018-926X(98)09691-4.

Hypothesis testing involves deciding among a set of alternatives (or hypotheses) based upon the observation of a set of random variables. This concept, which has been a topic studied by statisticians for many years, provides a mathematically solid foundation to perform target identification. By combining this concept with an SEM representation of the scattered field, we develop a mathematically rigorous formulation of generalized hypothesis testing to perform target identification. This formulation is based on a set of known poles $\{s_i\}$ and a set of unknown amplitudes $\{a_i\}$. In addition to the mathematical development, numerous results are provided demonstrating the effectiveness of the generalized likelihood ratio test. These results, which are shown as percent correct identification versus signal-to-noise ratio (SNR), contrast the performance of the generalized likelihood ratio test (GLRT) to the E-pulse filter technique.

II. Problem Formation

The problem of interest here is to identify a specific target based on the scattered field returned from a "wide-band" transmitted pulse. In order to simplify this problem, several assumptions are made. First, we assume that a target has been detected and only a single target is responsible for the returned scattered field. Furthermore, we assume that the target generating the return belongs to a group of targets for which we know *a priori* the poles of each. Based on these assumptions, we will develop a generalized likelihood ratio test to discriminate among a set of M known targets.

As mentioned previously, the concept of using a target's poles to perform target ID is based on the singularity expansion method (SEM) representation of the transient scattered field returned from a target that has been illuminated by an "impulsive" (wide bandwidth) radar pulse. Assuming a target exists and its from a family of M possible candidates, then the SEM representation of the return from the kth target in the presence of noise can be written as

$$y(t) = \sum_{i=1}^{N} a_i^{(k)} b_i^{(k)}(t) + n(t) \qquad t > T_L, \quad 1 \le k \le M \quad (2)$$

where

$$b_i^{(k)}(t) = e^{s_i^{(k)} t}$$

and $n(t)$ is additive white Gaussian noise with zero mean and variance σ^2. The equation in (2) leads to the major question addressed in this paper. That is, if we know the target belongs to the family of M targets and we know the poles of the target, then what is the likelihood the target generated the return $y(t)$?

III. Algorithm Development

A. Discretization

For convenience as well as for practical implementation using digital signal processing (DSP) hardware, we denote the various signals in (2) by their uniform samples at the interval T_s:

$$\mathbf{y} \equiv \begin{bmatrix} y(T_L) \\ y(T_L+T_s) \\ y(T_L+2T_s) \\ \vdots \end{bmatrix}; \qquad \mathbf{b}_i^k \equiv \begin{bmatrix} b_i^{(k)}(T_L) \\ b_i^{(k)}(T_L+T_s) \\ b_i^{(k)}(T_L+2T_s) \\ \vdots \end{bmatrix};$$

$$\mathbf{n} \equiv \begin{bmatrix} n(T_L) \\ n(T_L+T_s) \\ n(T_L+2T_s) \\ \vdots \end{bmatrix}.$$

Thus, the return signal vector $\mathbf{y}$ under target k becomes

$$H_k\colon \quad \mathbf{y} = \mathbf{B}_k \mathbf{a}_k + \mathbf{n} \quad (3)$$

where the unknown vector is

$$\mathbf{a}_k \equiv [a_1^k \quad a_2^k \quad a_3^k \quad \cdots \quad a_N^k]^T$$

and the known signal modes are

$$\mathbf{B}_k \equiv [\mathbf{b}_1^k \quad \mathbf{b}_2^k \quad \cdots \quad \mathbf{b}_N^k].$$

For the analysis presented here, $\mathbf{a}_k$ is an unknown parameter vector in the identification of target k. The only known parameters are the poles which determine $\mathbf{B}_k$ and the measured return $\mathbf{y}$. Our task is to construct a robust detection method to determine which of the M known targets is most likely to generate the received noisy signal $\mathbf{y}$ that depends on an unknown vector $\mathbf{a}$.

B. Generalized Hypothesis Testing

Without loss of generality, a Bayes criterion can be used to develop a likelihood ratio test (LRT) [15] to decide between targets 1 and 2. The LRT is written in terms of the likelihood functions as

$$\text{LRT:} \quad \frac{p(\mathbf{y}|\text{target } 1)}{p(\mathbf{y}|\text{target } 2)} \underset{H_2}{\overset{H_1}{\gtrless}} \gamma. \quad (4)$$

Since the noise has been characterized as being white and Gaussian, the likelihood function for the kth target is proportional to

$$p(\mathbf{y}|\text{target } k) \propto \exp\left(-\frac{1}{2\sigma^2}(\mathbf{y}-\mathbf{B}_k\mathbf{a}_k)^H(\mathbf{y}-\mathbf{B}_k\mathbf{a}_k)\right). \quad (5)$$

The threshold γ is a function of the prior probabilities and the cost. If we assume that all targets are equally probable and when uniform cost (zero for a correct decision and one for an incorrect decision) is assumed, then $\gamma = 1$. For multiple targets ($M > 2$), multiple LRT's need to be tested.

Though the LRT is a very useful tool in a number of applications, target identification cannot benefit directly since orientation dependency results in the unknown parameter vector $\mathbf{a_k}$. An alternative solution is to use the generalized likelihood ratio test (GLRT) [15]. The GLRT can be written in a form similar to the LRT as

$$\text{GLRT:}\quad \frac{\max_{\mathbf{a}_1}\ p(\mathbf{y}|\text{target } 1)}{\max_{\mathbf{a}_2}\ p(\mathbf{y}|\text{target } 2)} \underset{H_2}{\overset{H_1}{\gtrless}} \gamma. \tag{6}$$

Maximizing the likelihood function

$$p(\mathbf{y}|\text{target } k) \propto \exp\left(-\frac{1}{2\sigma^2}(\mathbf{y}-\mathbf{B}_k\mathbf{a}_k)^H(\mathbf{y}-\mathbf{B}_k\mathbf{a}_k)\right)$$

is equivalent to minimizing $||\mathbf{y}-\mathbf{B}_k\mathbf{a}_k||^2$, hence yielding a least squares solution to $\mathbf{y}=\mathbf{B}_k\mathbf{a}_k$ as

$$\hat{\mathbf{a}}_{k,\max} = (\mathbf{B}_k^H\mathbf{B}_k)^{-1}\mathbf{B}_k^H\mathbf{y}. \tag{7}$$

Substituting the least-squares solution into the GLRT for the simple two target case (with $\gamma = 1$) yields after some manipulation the decision rule

$$\mathbf{y}^H\mathbf{B}_1(\mathbf{B}_1^H\mathbf{B}_1)^{-1}\mathbf{B}_1^H\mathbf{y} \underset{H_2}{\overset{H_1}{\gtrless}} \mathbf{y}^H\mathbf{B}_2(\mathbf{B}_2^H\mathbf{B}_2)^{-1}\mathbf{B}_2^H\mathbf{y}. \tag{8}$$

If we maintain the conditions of equal prior probabilities and uniform cost, then for multiple hypothesis testing, the above decision rule can be generalized for M target discrimination as

$$\text{decide } \{y(t)\} = \text{target } k \text{ if } \mathbf{y}^H\mathbf{B}_k(\mathbf{B}_k^H\mathbf{B}_k)^{-1}\mathbf{B}_k^H\mathbf{y} \text{ is maximum.} \tag{9}$$

IV. SUFFICIENT STATISTICS AND PRACTICAL CONSIDERATIONS

A. Real Time Implementation

Having developed a maximum likelihood (ML) decision rule to discriminate among a set of M targets, it is appropriate to introduce the concept of the "sufficient statistics." Generally, speaking, "sufficient statistics" represent those computations which are sufficient to make a decision as to which target is present. In other words, the sufficient statistics answer the question, "What minimal computations are required in order to decide which target is present?" Through some minor manipulation, the decision rule in (9) can be rewritten as follows:

$$\mathbf{y}^H\mathbf{B}_k(\mathbf{B}_k^H\mathbf{B}_k)^{-1}\mathbf{B}_k^H\mathbf{y} = ||(\mathbf{B}_k^H\mathbf{B}_k)^{-1/2}\mathbf{B}_k^H\mathbf{y}||^2 \tag{10}$$

where $||\cdot||$ denotes the vector 2-norm (or Euclidean norm). As one can see from (10), the GLRT is simply based upon the computation of $||(\mathbf{B}_k^H\mathbf{B}_k)^{-1/2}\mathbf{B}_k^H\mathbf{y}||$. Therefore, the sufficient statistics for the GLRT are $(\mathbf{B}_k^H\mathbf{B}_k)^{-1/2}$ and $\mathbf{B}_k\mathbf{y}$.

If hardware implementations on continuous time signals are necessary, these sufficient statistics can be written for continuous time signals as shown in (11) and (12), shown at the bottom of the page, where $W=[T_L, T)$ is the processing window. A closed-form solution exits for the integrals in the matrix $\mathbf{B}_k^H\mathbf{B}_k$ since the integrands are products of simple exponential terms. Thus, this allows $(\mathbf{B}_k^H\mathbf{B}_k)^{-1/2}\mathbf{B}_k^H$ to be precomputed and stored in memory as *a priori* knowledge. To summarize, the GLRT detector is simply

$$\text{decide}\{y(t)\} = \text{target } k \text{ if } ||(\mathbf{B}_k^H\mathbf{B}_k)^{-1/2}\mathbf{B}_k^H\mathbf{y}||^2 \text{ is maximum.} \tag{13}$$

The computation of the sufficient statistic $(\mathbf{B}_k^H\mathbf{B}_k)^{-1/2}\mathbf{B}_k^H$ is dependent on the processing window W. In our analysis, we assume the beginning of late-time to be twice the maximum transit time of the target. However, in a practical discrimination scheme, the beginning of the late-time must be estimated. As shown by Ilavarasan *et al.* [14], the beginning of late-time for backscattered responses is given by

$$T_L = T_b + T_p + 2T_{tr} \tag{14}$$

where T_{tr} is the maximum transit time of the target, T_p is the effective pulse duration used in the system, and T_b is an estimate of the time when the incident wave strikes the leading edge of the target. The time T_b is estimated based on a threshold voltage V_T which needs to be large enough to detect small signals, but small enough to maintain a small false alarm rate. Under a Gaussian noise assumption, V_T can be calculated for a desired mean time between false alarms [16]. The end-time T can be chosen so that 99% of the noise-free signal energy is contained within the processing window [14].

B. Computational Complexity

Based on the sufficient statistics introduced above, the computational complexity of the GLRT algorithm can be investigated. If we assume that each target in the library has N poles and that the received signal $\mathbf{y}$ is sampled Q times, then

$$\mathbf{B}_k^H\mathbf{y} = \begin{bmatrix} \mathbf{b}_1^{(k)^H}\mathbf{y} \\ \mathbf{b}_2^{(k)^H}\mathbf{y} \\ \vdots \\ \mathbf{b}_N^{(k)^H}\mathbf{y} \end{bmatrix} = \begin{bmatrix} \int_W y(t)b_1^{(k)*}(t)\,dt \\ \int_W y(t)b_2^{(k)*}(t)\,dt \\ \vdots \\ \int_W y(t)b_N^{(k)*}(t)\,dt \end{bmatrix} \tag{11}$$

$$\mathbf{B}_k^H\mathbf{B}_k = \begin{bmatrix} \int_W b_1^{(k)}(t)b_1^{(k)*}(t)\,dt & \int_W b_2^{(k)}(t)b_1^{(k)*}(t)\,dt & \cdots & \int_W b_N^{(k)}(t)b_1^{(k)*}(t)\,dt \\ \int_W b_1^{(k)}(t)b_2^{(k)*}(t)\,dt & \int_W b_2^{(k)}(t)b_2^{(k)*}(t)\,dt & \cdots & \int_W b_N^{(k)}(t)b_2^{(k)*}(t)\,dt \\ \vdots & \vdots & \ddots & \vdots \\ \int_W b_1^{(k)}(t)b_N^{(k)*}(t)\,dt & \int_W b_2^{(k)}(t)b_N^{(k)*}(t)\,dt & \cdots & \int_W b_N^{(k)}(t)b_N^{(k)*}(t)\,dt \end{bmatrix} \tag{12}$$

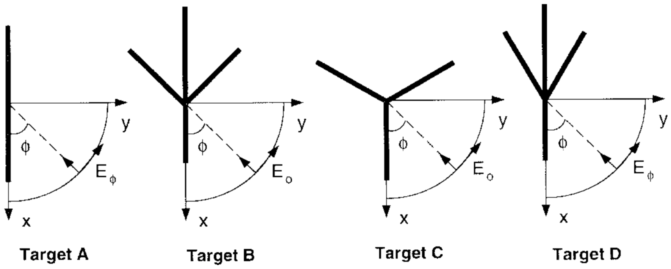

Fig. 1. Targets A, B, C, and D used in the simulations to demonstrate the performance of the GLRT and E-pulse technique.

the size of the sufficient statistic $(\mathbf{B}_k^H\mathbf{B}_k)^{-1/2}\mathbf{B}_k^H$ is $N \times Q$. Multiplying this quantity by $\mathbf{y}$ requires NQ multiplications and $N(Q-1)$ additions and yields a vector of length N. Performing the Euclidean norm operation as shown in (13) requires an additional N multiplies and $N-1$ additions. Thus, to compute (13) for a single target requires a total of $N(Q+1)$ multiplications and $NQ-1$ additions. If we have M targets, then in order to yield a decision, a total of $MN(Q+1)$ multiplications and $M(NQ-1)$ additions must be performed.

The number of calculations required to render a decision via the E-pulse technique are approximately the same required by the GLRT. However, in the E-pulse technique, each E-pulse filter is essentially a digital filter with its own sampling rate. This feature is due to the construction of an E-pulse filter for each individual target and involves the resonances of each target [8], [17]. Thus, if we have M targets, then we need M different samplers. This obviously increases the preprocessing time before a decision can be made and, furthermore, it undoubtedly makes the system more complicated and expensive.

V. Simulation Results

A. Experimental Setup

To demonstrate the effectiveness of the GLRT as a function of signal-to-noise ratio (SNR), several simulations were conducted using the four targets shown in Fig. 1. Target A is a simple 1-m-long thin cylinder lying along the x axis and centered at the origin. Target B is a swept wing aircraft model. This example was chosen for its obvious relevance to target identification (ID). The fuselage of the aircraft lies along the x axis with forward and aft sections of 1/3 and 2/3 m, respectively. The wings are swept back 45° from the normal to the fuselage and are 1/2 m in length. Target C is a perturbed symmetric tripole. Two of the arms are each a length of 1/2 m, and the third arm has a length of 0.5238 m. Target D is also a swept wing aircraft model similar to Target B. The only distinguishing feature between the two is the angle at which the wings are swept back. The wings on Target D are swept back 60° from the normal to the fuselage. Also shown in Fig. 1 is the orientation of the incident field E_ϕ relative to each target.

The scattering data used in the experiment are the theoretical impulse responses of the four targets mentioned above. These responses were obtained using the SEM, which was cast into

TABLE I
THE NATURAL FREQUENCIES OF THE FOUR TARGETS USED IN THE SIMULATION

$\frac{s_{m,n}l}{c}$	Thin Cylinder		45° Swept Wing		Perturbed Tripole		60° Swept Wing	
m,n	Real	Imag.	Real	Imag.	Real	Imag.	Real	Imag.
1,1	-0.2574	± 2.8743	-0.1142	± 2.6857	-0.2123	± 2.8645	-0.1320	± 2.7726
1,2	-0.3792	± 5.9329	-0.1748	± 3.0526	-0.2205	± 2.9538	-0.1149	± 3.2110
1,3	-0.4660	± 9.0117	-0.3215	± 3.6096	-0.2689	± 6.2325	-0.2992	± 3.5114
1,4	-0.5353	± 12.0955	-0.4772	± 6.6065	-0.5025	± 9.2240	-0.6288	± 6.5274
1,5	-0.5935	± 15.1775	-0.4059	± 7.9230	-0.4821	± 8.9461	-0.3005	± 7.9773
1,6	-0.6436	± 18.2533	-0.6182	± 9.3581	-0.4637	± 12.5192	-0.6102	± 9.3557
1,7	-0.6870	± 21.3193	-0.5594	± 11.0463	-0.7218	± 15.0031	-0.5647	± 11.0262
1,8	-0.7244	± 24.3726	-0.5560	± 12.0588	-0.7552	± 15.4586	-0.4928	± 12.0233
1,9	******	******	-0.5882	± 14.8595	-0.7043	± 18.6706	-0.7045	± 14.6847
1,10	******	******	-0.8985	± 15.4281	-0.9387	± 20.9337	-0.6975	± 15.6535
1,11	******	******	-0.6356	± 16.4076	-0.9835	± 21.5461	-0.4349	± 16.5412
1,12	******	******	-0.7755	± 18.7524	-0.9383	± 24.5863	-0.8272	± 18.6455
1,13	******	******	-0.6201	± 21.1990	******	******	-0.6110	± 21.2738
1,14	******	******	-0.9542	± 21.5145	******	******	-0.9544	± 21.7441
1,15	******	******	-0.7550	± 22.3478	******	******	-0.6915	± 22.1412

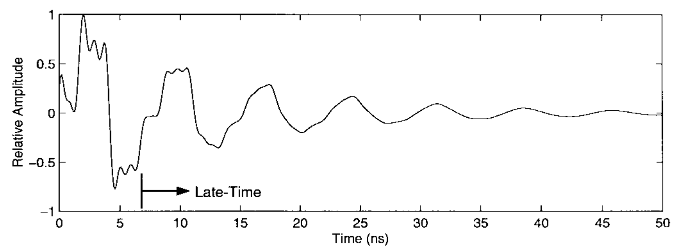

Fig. 2. The backscattering response of the thin wire (Target A) due to an impulsive plane wave incident from $\phi = 75°$.

numerical form via the method of moments. The poles that were used in obtaining the back scattered field from each target are listed in Table I. The first eight complex conjugate pole pairs were used in computing the backscattered field impulse response of the 1-m-thin cylinder. In order to ensure that the same bandwidth was used among each of the four targets, it was necessary to use the first 15 conjugate poles pairs to compute the impulse response of the 45° and 60° swept wing aircraft models. Similarly, the first twelve poles of the perturbed symmetric tripole were used in computing its impulse response. Fig. 2 shows the backscattering response of the thin cylinder (target A) due to an impulsive plane wave incident from $\phi = 75°$. It should be noted here that the impulse responses for all targets were computed using a Class I coupling coefficient; thus, the early-time portion of the responses are inaccurate.

The experimental setup for the simulation process is illustrated in Fig. 3. In each simulation, a computer randomly selects one of the targets from the target library. The selection process is conditioned by the assumption that each target has an equal probability of being present. Recall this assumption was used in the development of the GLRT detector. In the results to be presented here, two different simulations were performed. One simulation involves only targets A, B, and C. In the remaining simulation, all four targets are used. Thus, in the simulation involving three targets, each target has a 1/3 probability of being selected. Similarly, each target has a probability of 1/4 of being selected in the simulation involving four targets.

Once a target has been selected, white Gaussian noise is added to a corresponding signature $(r(t))$ of the selected target. The value of the average noise power σ^2 is adjusted accordingly for a specified SNR (in decibels) through the

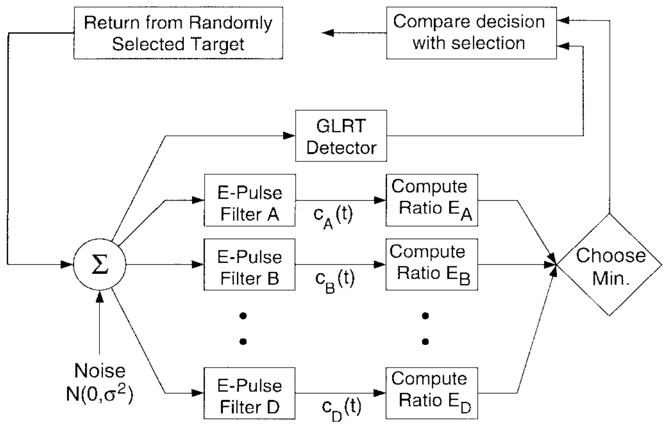

Fig. 3. The experimental setup for demonstrating the performance of the GLRT and comparing it to the E-pulse filter technique.

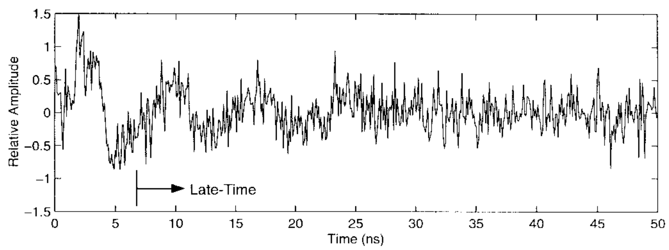

Fig. 4. The backscattering impulse response of the thin wire (Target A) for $\phi = 75^\circ$ and an SNR of 0 dB.

relationship

$$\sigma^2 = P_{\rm sig} 10^{-{\rm SNR}/10} \tag{15}$$

where $P_{\rm sig}$ is the average power of the uncorrupted signature $r(t)$ and is defined as

$$P_{sig} = \frac{1}{T}\int_0^T r^2(t)\,dt. \tag{16}$$

Note the average power of the signature $P_{\rm sig}$ is computed using both the early-time and late-time portions of the return. The end-time T of the integration is arbitrarily chosen to be 50 ns. Fig. 4 shows the backscattering response from the thin wire for $\phi = 75^\circ$ and an SNR of 0 dB.

After adding the noise to the signature $r(t)$, the corrupted return is then given to the GLRT detector, which renders a decision as to which target is present. This process is repeated 1000 times at *each* specified value of SNR. For the purposes of this experiment, the SNR values are chosen to range from −25 to 35 dB.

B. E-Pulse Filter Design

Also shown in Fig. 3 is the scheme by which the performance of the GLRT is compared to E-pulse filter technique. In this scheme, an energy ratio [18] is computed at the output of each E-pulse filter. For example, the energy ratio to be

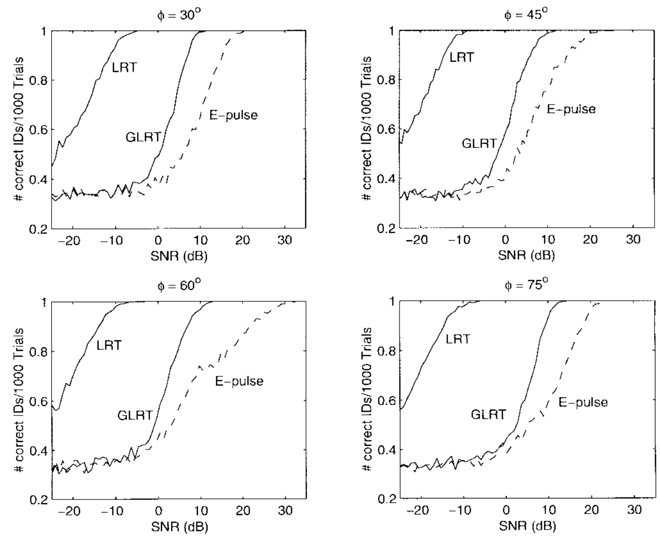

Fig. 5. The performance of the GLRT, LRT, and E-pulse filter technique as a function of SNR for different aspect angles using targets A, B, and C.

computed at the output of E-pulse filter A is defined as

$$E_A = \frac{\displaystyle\int_{T_{{\rm LES}_A}}^{T_{{\rm LEE}_A}} c^2(t)\,dt}{\displaystyle\int_0^{T_{e_A}} e_A^2(t)\,dt}. \tag{17}$$

The parameter $c(t)$ represents the convolution of the E-pulse $e_A(t)$ with the received return. If $c(t)$ is the correct target (Target A), then ideally the energy ratio would be zero. The time $T_{{\rm LES}_A}$ is defined as

$$T_{{\rm LES}_A} = T_{e_A} + 2T_{L_A} \tag{18}$$

and represents the "earliest time at which the unknown target convolution is certain to be a unique series of natural modes" [18]. The time T_{e_A} is the duration of the E-pulse for Target A, and $T_{{\rm LEE}_A}$ is the end time of the energy ratio. In general, the time $T_{\rm LEE}$ is selected so that the window length $T_{\rm LEE} - T_{\rm LES}$ is the same for each ratio. For the simulations presented here, a window length of 15 ns was used. A correct identification is determined by the minimum energy ratio at the output of the E-pulse of the unknown target. For example, if the energy ratio at the output of the E-pulse filter for Target A is the smallest, then Target A is selected to be the correct target.

C. Results

Of the two simulations performed, the first involves only targets A, B, and C. The results of this simulation are shown in Fig. 5 for various target orientations. For each target orientation, the performance of the GLRT, LRT, and E-pulse technique are plotted as a function of SNR in decibels. The performance of each method is defined as the number of correct identifications per 1000 trials at a specified value of SNR.

The LRT is included in the results in order to provide an upper bound on the performance of the GLRT. In the LRT, the poles as well as the coupling coefficients of each target are know *a priori* whereas in the GLRT, only the poles of each

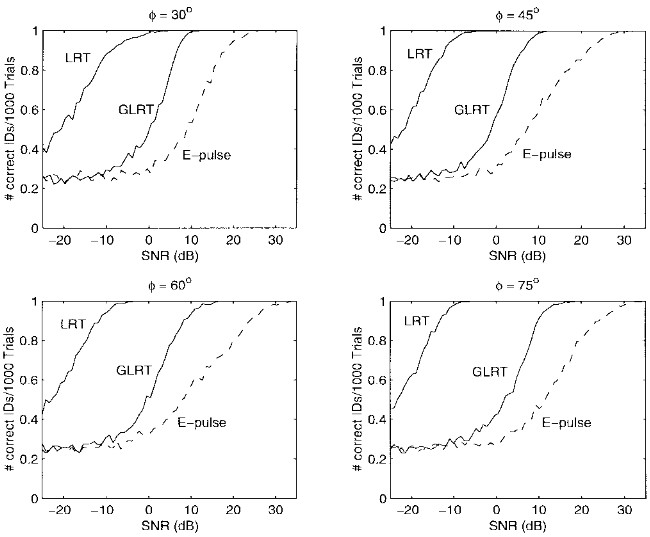

Fig. 6. The performance of the GLRT, LRT, and E-pulse filter technique as a function of SNR for different aspect angles using targets A, B, C, and D.

target are known. Because the LRT utilizes more information in the identification process, it clearly out performs both the GLRT and E-pulse technique by a significant margin. In each of the aspect angles considered here, the LRT begins to identify the correct target in every trial at approximately −6 dB of SNR. Note that at very low values of SNR, the confidence level of the GLRT is very low. At these values, the GLRT detector correctly identifies the target only 33% of the time. This result is consistent with the condition that each target has an equal probability of being present. Thus, when the SNR is very low, the best the GLRT detector can do is conditioned by what is know about the targets beforehand.

The difference in performance between the GLRT and E-pulse technique varied with aspect angle. At an aspect angle of 30°, the GLRT begins to correctly identify the target in every trial at an SNR of approximately 12 dB. This same level of performance does not occur with the E-pulse technique until the SNR reaches approximately 22 dB. Thus, there is a 10 dB difference in SNR for the same level of performance between the two methods at a target orientation of 30°. This difference in performance is observed to increase for the other aspect angles considered. In the case where the aspect angle is 60°, the difference in performance exceeds well over 20 dB in SNR.

The results of the second simulation, which involved targets A, B, C, and D, are similar to those obtained in the three target simulation. These results are shown in Fig. 6 for four different target orientations. In all the target orientations considered, the LRT out performed both the GLRT and E-pulse technique by a considerable margin as expected. Furthermore, at very low SNR values, the GLRT detector identifies the correct target only 25% of the time. As was observed in the previous simulation, this is consistent with the condition that each target has an equal prior probability of being selected.

As expected, the performance of the GLRT and E-pulse technique increase with increasing SNR. However, the difference in performance between the two methods varied with aspect angle. At an aspect of 30°, the GLRT detector begins to correctly identify the target in every trial at an SNR value of 13 dB. The E-pulse technique does not equal this performance until the SNR reaches 27 dB. Thus, for this aspect angle, there is roughly a 14-dB difference in SNR for the same level performance between the two methods. In the other aspect angles considered, this difference in performance exceeds 15 dB in SNR and reaches 17 dB in the case where the aspect angle is 60°. Nevertheless, it should be noted that in all of our simulation tests, GLRT consistently outperforms the E-pulse technique.

VI. Conclusions

In this paper, we have used well-established mathematical models and rigorous statistical analysis to develop a simple but reliable method to perform target identification. Beginning with an SEM representation of the scattered field, we have developed a detector based on a GLRT that is capable of identifying a specific target out of a family of M candidates. The GLRT assumes only a knowledge of a target's natural resonances thereby making the method aspect independent.

A number of numerical results were presented demonstrating the effectiveness of the GLRT in the presence of random noise. These results showed the ability of the GLRT to identify the correct target at low SNR values. Furthermore, the GLRT was compared to the E-pulse technique. In the simulations we performed, the GLRT out performed the E-pulse method by a considerable margin.

References

[1] C. E. Baum, "On the singularity expansion method for the solution of electromagnetic interaction problems," Air Force Weapons Lab, Interaction Note 88, 1971.

[2] ——, "Scattering, reciprocity, symmetry, EEM, and SEM," Air Force Weapons Lab, Interaction Note 475, 1989.

[3] ——, "SEM backscattering," Air Force Weapons Lab, Interaction Note 476, 1989.

[4] ——, "Representation of surface current density and far scattering in EEM and SEM with entire functions," Phillips Laboratory, Kirkland AFB, Interaction Note 486, 1992.

[5] M. A. Richards, "SEM representation of the early and late time fields scattered from wire targets," *IEEE Trans. Antennas Propagat.*, vol. 42, pp. 564–566, Apr. 1994.

[6] L. W. Pearson, M. J. Blaricum, and R. Mittra, "A new method for radar target recognition based upon the singularity expansion method," in *Rec. IEEE Int. Radar Conf.*, Arlington, VA, Apr. 1975, pp. 452–457.

[7] M. V. Blaricum and R. Mittra, "A technique for extracting the poles and residues of a system directly from its transient response," *IEEE Trans. Antennas Propagat.*, vol. AP-23, pp. 777–781, Nov. 1975.

[8] E. Rothwell, D. P. Nyquist, K. M. Chen, and B. Drachman, "Radar target discrimination using the extinction-pulse technique," *IEEE Trans. Antennas Propagat.*, vol. AP-33, pp. 929–937, Sept. 1985.

[9] K. M. Chen, D. P. Nyquist, E. J. Rothwell, L. L. Webb, and B. Drachman, "Radar target discrimination by convolution of radar returns with extinction pulses and single-mode extraction signals," *IEEE Trans. Antennas Propagat.*, vol. AP-34, pp. 896–904, July 1986.

[10] E. M. Kennaugh, "The K-pulse concept," *IEEE Trans. Antennas Propagat.*, vol. AP-35, pp. 327–331, Mar. 1981.

[11] F. Y. S. Fok and D. Moffat, "The K-pulse and E-pulse," *IEEE Trans. Antennas Propagat.*, vol. AP-35, pp. 1325–1326, Nov. 1987.

[12] E. J. Rothwell, K. M. Chen, and D. P. Nyquist, "Extraction of the natural frequencies of a radar target from a measured response using e-pulse techniques," *IEEE Trans. Antennas Propagat.*, vol. AP-35, pp. 715–720, June 1987.

[13] J. P. R. Bayard and D. H. Schaubert, "Target identification using optimization techniques," *IEEE Trans. Antennas Propagat.*, vol. 38, pp. 450–456, Apr. 1990.

[14] P. Ilavarasan, J. E. Ross, E. J. Rothwell, K. M. Chen, and D. P. Nyquist, "Performance of an automated radar target discrimination scheme using E pulses and S pulses," *IEEE Trans. Antennas Propagat.*, vol. 41, pp. 582–588, May 1993.

[15] H. L. Van Trees, *Detection, Estimation, and Modulation Theory: Part I.* New York: Wiley, 1967.

[16] M. L. Skolnik, *Introduction to Radar Systems.* New York: McGraw-Hill, 1980.

[17] E. J. Rothwell, K. M. Chen, D. P. Nyquist, and W. Sun, "Frequency domain E-pulse synthesis and target discrimination," *IEEE Trans. Antennas Propagat.*, vol. AP-35, pp. 426–434, Apr. 1987.

[18] C. E. Baum, E. J. Rothwell, K. M. Chen, and D. P. Nyquist, "The singularity expansion method and its application to target identification," *Proce. IEEE*, pp. 1481–1492, Oct. 1991.

Jon E. Mooney (S'94) was born in Montgomery, AL, on July 2, 1970. He received the B.E.E. (*summa cum laude*) and M.S. degrees in electrical engineering from Auburn University, Auburn, AL, in 1993 and 1996, respectively. He is currently working toward the Ph.D. degree in electrical engineering from Auburn University.

From 1993 to 1996, he was a United States Air Force Laboratory Graduate Fellow. His research interests include computational electromagnetics as well as statistical signal processing with application to radar target identification.

Mr. Mooney is a member of Eta Kappa Nu, Tau Beta Pi, and Phi Kappa Phi.

Zhi Ding (M'87–SM'95) was born in Harbin, China. He received the B.Eng. degree in 1982 from the Department of Wireless Engineering, Nanjing Institute of Technology, Nanjing, China, the M.A.Sc. degree from the Department of Electrical Engineering, University of Toronto, Toronto, Canada, in 1987, and the Ph.D. degree from the School of Electrical Engineering, Cornell University, Ithaca, NY, in 1990.

He joined the faculty of Auburn University, Auburn, AL, in 1990 where he is currently an Associate Professor in the Department of Electrical Engineering. He has held visiting positions in the Australian National University, the Hong Kong University of Science and Technology, the NASA Lewis Research Center, and the USAF Wright Laboratory. His main research interests include digital communications, signal detection, adaptive signal processing, blind equalization, and cyclostationary signal processing.

Lloyd S. Riggs (SM'98) received the Ph.D. degree from Auburn University, Auburn, AL, in 1985.

Prior to receiving the Ph.D. degree, he spent three years as an Antenna Design Engineer with the Electronics Systems Division at Harris Corporation in Palm Bay, FL. While at Harris, he was involved in the design of frequency selective surfaces (FSS) with application to dual and multiband radomes and satellite antennas. He was also involved in the synthesis of space-borne reflector antenna configurations for military communication and commercial direct broadcast contoured beam applications. Since the end of 1983, he has worked in the Electrical Engineering Department at Auburn University, AL. In this capacity he has been the Principal Investigator on a variety of research projects with both industry and government. He has worked with the Antenna Group of Raytheon Systems Corporation (formerly Texas Instruments), McKinney, TX, using the transmission-line matrix method (TLM) of numerical analysis to develop algorithms useful in the analysis and design of microwave devices. He has also worked with the Jet Propulsion Laboratory (JPL), Pasadena, CA, using TLM to design a stepped-septum polarizer for the Cassini (Saturn Orbiter/Titan Probe) mission. He consults with the United States Army Missile Command in Huntsville, AL, and in this capacity has been involved in research to identify targets based on their high-range resolution (HRR) radar signatures. He is interested in electromagnetic-based sensors [ground penetrating radar (GPR)] for the detection and identification of buried anomalies (mines). He is currently working witht the United States Army's Night Vision Laboratory in Belvoir, VA, using the low-frequency quasi-magnetostatic response of finitely conducting objects to reduce false alarms in metal detectors. He is presently serving as the Major Professor for three master's and one Ph.D. candidate. Since 1983, he has served as the Major Professor for over 18 graduate students. He has published more than 20 referred journal articles and 30 conference papers.

Dr. Riggs received the Best Paper of the Year Award (with T. H. Shumpert and J. Lindsey) in the IEEE TRANSACTIONS ON ELECTROMAGNETIC COMPATIBILITY for "Intermodulation Effects on Parallel Wires by Transient Excitation" in 1990.